Priority Research Paper

Green tea catechins EGCG and ECG enhance the fitness and lifespan of *Caenorhabditis elegans* by complex I inhibition

Jing Tian[1,2], Caroline Geiss[1], Kim Zarse[1,3], Corina T. Madreiter-Sokolowski[3,4], Michael Ristow[1,3]

[1]Department of Human Nutrition, Institute of Nutrition, Friedrich Schiller University Jena, Jena 07743, Germany
[2]MOE Key Laboratory of Environment Correlative Dietology, College of Food Science and Technology, Huazhong Agricultural University, Wuhan 430070, China
[3]Laboratory of Energy Metabolism, Institute of Translational Medicine, Department of Health Sciences and Technology, ETH Zurich, Schwerzenbach 8603, Switzerland
[4]Molecular Biology and Biochemistry, Gottfried Schatz Research Center, Medical University of Graz, Graz 8010, Austria

Correspondence to: Corina T. Madreiter-Sokolowski, Michael Ristow; **email:** corina.madreiter@medunigraz.at, michael-ristow@ethz.ch
Keywords: aging, reactive oxygen species, mitochondria, polyphenols, *C. elegans*
Received: July 8, 2021 **Accepted:** September 25, 2021 **Published:** October 4, 2021

ABSTRACT

Green tea catechins are associated with a delay in aging. We have designed the current study to investigate the impact and to unveil the target of the most abundant green tea catechins, epigallocatechin gallate (EGCG) and epicatechin gallate (ECG).

Experiments were performed in *Caenorhabditis elegans* to analyze cellular metabolism, ROS homeostasis, stress resistance, physical exercise capacity, health- and lifespan, and the underlying signaling pathways. Besides, we examined the impact of EGCG and ECG in isolated murine mitochondria.

A concentration of 2.5 µM EGCG and ECG enhanced health- and lifespan as well as stress resistance in *C. elegans*. Catechins hampered mitochondrial respiration in *C. elegans* after 6–12 h and the activity of complex I in isolated rodent mitochondria. The impaired mitochondrial respiration was accompanied by a transient drop in ATP production and a temporary increase in ROS levels in *C. elegans*. After 24 h, mitochondrial respiration and ATP levels got restored, and ROS levels even dropped below control conditions. The lifespan increases induced by EGCG and ECG were dependent on AAK-2/AMPK and SIR-2.1/SIRT1, as well as on PMK-1/p38 MAPK, SKN-1/NRF2, and DAF-16/FOXO. Long-term effects included significantly diminished fat content and enhanced SOD and CAT activities, required for the positive impact of catechins on lifespan.

In summary, complex I inhibition by EGCG and ECG induced a transient drop in cellular ATP levels and a temporary ROS burst, resulting in SKN-1 and DAF-16 activation. Through adaptative responses, catechins reduced fat content, enhanced ROS defense, and improved healthspan in the long term.

INTRODUCTION

Clinical trials and epidemiological studies have revealed health benefits associated with green tea consumption, including a significant reduction in systolic blood pressure [1] and fasting glucose [2] as well as weight loss in type 2 diabetes patients [3] and in women with central obesity [4]. The most abundant polyphenols in green tea leaves are epigallocatechin gallate (EGCG), epicatechin gallate (ECG), epigallocatechin (EGC), and epicatechin (EC), forming 30–42% of the solid green tea extract [5]. EGCG accounts for roughly 50% and ECG for 20% of the total catechin amount in green tea leaves [6]. A randomized, placebo-controlled clinical trial testing a daily

supplementation with 400 mg EGCG confirmed the safety of a one-year administration with EGCG. It revealed further that plasma concentrations of EGCG reached a measurable level after six months [7]. A recent study tested the bioavailability of EGCG combined with various food supplements. After overnight fasting, consumption of 150 mg green tea extracts already resulted in plasma level peaks of 10 ng/ml/kg after 60–180 min [8]. *In vivo* experiments in various model organisms suggested a beneficial effect of green tea catechins on lifespan due to metabolic adaptation and enhanced resistance to reactive oxygen species (ROS). For instance, dietary supplementation with EGCG-rich green tea extracts (10 mg/ml EGCG) affected glucose metabolism and increased health- and lifespan in *Drosophila melanogaster* [9]. Besides, green tea polyphenol-containing water (80 mg/l) extended the lifespan of male C57BL/6 mice [10]. Moreover, treatment of *Caenorhabditis elegans (C. elegans)* with EGCG at concentrations of 50–300 μM during early-to-mid adulthood promoted lifespan, and 200 μM EGCG was the most potent dosage to extend lifespan via inducing a *mitohormetic* response via AMPK/SIRT1 and FOXO [11].

However, the poor bioavailability of green tea catechins in mammals [12, 13] makes it unlikely to achieve this concentration after oral administration in humans. Nevertheless, several independent clinical trials confirmed that green tea consumption improves various health parameters [1–4]. After administration of a maximum of 4.5 g of decaffeinated green tea solids, maximum plasma concentrations of EGCG, ECG, and EC reached in total roughly 2.5 μM in humans [14]. Consequently, we tested whether 2.5 μM is still sufficient to promote lifespan by inducing a *mitohormetic* response in *C. elegans.* In this work, we reveal that EGCG and ECG enhance fitness and increase the lifespan of *C. elegans* already at a concentration of 2.5 μM. This comparably low dosage is sufficient to inhibit the mitochondrial respiration chain activity in *C. elegans.* Experiments in isolated murine liver mitochondria revealed that EGCG and ECG hamper complex I activity. Inhibition of complex I was accompanied by transient ROS formation and an ATP drop after 6 h of EGCG and 12 h of ECG treatment in *C. elegans*. Lifespan extension of *C. elegans* by EGCG and ECG proved to be dependent on the presence of the energy sensors AMP-activated kinase AAK-2 and NAD-dependent protein deacetylase SIR-2.1, the homologs of mammalian AMPK and SIRT1, as well as on the ROS-sensing mitogen-activated protein kinase PMK-1, the orthologue of mammalian mitogen-activated protein kinase p38 MAPK, and in the following on its downstream targets protein skinhead-1 (SKN-1), the orthologue of nuclear factor erythroid 2-related factor 2 (NRF2), and DAF-16, the orthologue of a mammalian forkhead transcription factor (FOXO). These data suggest that the subsequent energy deficiency due to transient AMP drop triggers the energy sensors AAK-2 and SIR-2.1 in *C. elegans*. Moreover, the temporary increase in ROS levels might boost PMK-1 activity and, thereby, the respective signaling cascade, including SKN-1 and DAF-16 in *C. elegans.* Consistent with the concept of *mitohormesis*, these signaling pathways provoked an adaptive response by enhancing the activity of ROS defense enzymes superoxide dismutase (SOD) and catalase (CTL), increasing oxidative stress resistances, health, and lifespan. Moreover, metabolism changed in the long term, causing significantly reduced fat content in *C. elegans.* Taken together, inhibition of mitochondrial complex I once again proved to be a powerful tool to stimulate lifespan extension pathways.

RESULTS

EGCG and ECG promote lifespan, fitness, and stress resistance when applied at low doses

Oral absorption and absolute bioavailability of green tea catechins are low in mammals [12], reaching total maximum plasma concentrations of 2.5 μM in humans after administration of maximal 4.5 g of decaffeinated green tea solids [14]. However, several independent clinical trials reported beneficial effects of EGCG and ECG regarding health parameters [1–4]. Therefore, we hypothesized that lower concentrations of EGCG and ECG than those studied previously [11] are still effective and improve lifespan and stress resistance in *C. elegans.* Indeed, EGCG and ECG applied at a concentration of 2.5 μM were sufficient to significantly extend the medium lifespan (Table 1) of *C. elegans* from 28.8 ± 0.3 to 30.8 ± 0.1 days (Figure 1A) and from 28.8 ± 0.3 to 30.6 ± 0.3 days (Figure 1B), respectively, causing an extension of 6.9% for EGCG and 6.2% for ECG treatment. The maximum lifespan (Table 1) was extended from 35.7 ± 0.6 to 36.9 ± 0.1 days by EGCG treatment (Figure 1A) and from 35.7 ± 0.6 to 37.1 ± 0.3 days by ECG treatment (Figure 1B), reaching an extension of 3.4% for EGCG and 3.9% for ECG. Next, we tested whether prolonged lifespan also correlates with improved fitness and stress resistance. Locomotion is dependent on functional muscle mass, connective tissues, and neuronal signaling. Consequently, motility is a suitable marker for health [15]. EGCG and ECG treatment improved the nematodes' motility after 7 days of incubation (Figure 1C). Moreover, treatment of *C. elegans* with ECGC (Figure 1D) and ECG (Figure 1E) for 7 days significantly increased stress resistance (Table 2) to the free radical generator paraquat. Consequently, EGCG and ECG enhanced fitness and stress resistance, both crucial parameters for health.

Table 1. Lifespan results and statistical analysis.

Strains, Compounds	Max lifespan in days ± SD (10th percentile)	Medium lifespan in days ± SD (50th percentile)	Number of experiments (*n*)	*P* value versus control	Number of nematodes
N2 DMSO	35.7 ± 0.6	28.8 ± 0.3	18		2831
N2 EGCG	36.9 ± 0.1	30.8 ± 0.1	18	<0.0001	2842
N2 ECG	37.1 ± 0.3	30.6 ± 0.3	15	<0.0001	2777
N2 BHA	36.4 ± 0.6	28.9 ± 0.4	9	0.3838	1548
N2 BHA + EGCG	36.0 ± 0.3	29.2 ± 0.4	9	0.3114	1581
N2 BHA + ECG	35.9 ± 0.5	29.6 ± 0.4	6	0.6682	1451
***aak-2 (ok524)* DMSO**	24.2	20.9 ± 0.2	3		462
***aak-2 (ok524)* EGCG**	24.4 ± 0.2	20.5 ± 0.3	3	0.1015	465
***aak-2 (ok524)* ECG**	24.6 ± 0.7	20.4 ± 0.4	3	0.9876	452
***sir-2.1 (ok434)* DMSO**	28.6 ± 0.1	24.3 ± 0.4	3		400
***sir-2.1 (ok434)* EGCG**	28.9 ± 1.2	24.5 ± 0.3	3	0.1858	355
***sir-2.1 (ok434)* ECG**	28.2 ± 0.5	23.7 ± 0.1	3	0.24	436
***pmk-1 (km25)* DMSO**	34.9 ± 0.6	27.9 ± 0.4	3		548
***pmk-1 (km25)* EGCG**	35.5 ± 1.5	28.2 ± 1.1	3	0.7759	567
***pmk-1 (km25)* ECG**	35.3 ± 0.7	28.0 ± 0.3	3	0.7363	581
***skn-1 (zu67)* DMSO**	16.5 ± 0.5	14.1 ± 0.1	6		424
***skn-1 (zu67)* EGCG**	17.0 ± 0.2	14.2 ± 0.1	6	0.5286	432
***skn-1 (zu67)* ECG**	16.8 ± 0.2	14.3	6	0.4823	440
***daf-16 (mgDF47)* DMSO**	22.5 ± 0.3	20.1 ± 0.1	3		660
***daf-16 (mgDF47)* EGCG**	22.2 ± 0.2	19.8	3	0.029	774
***daf-16 (mgDF47)* ECG**	21.7 ± 0.6	19.4 ± 0.2	3	<0.0001	707
***sod-2 (gk257)* DMSO**	33.3 ± 0.4	27.2 ± 0.4	3		730
***sod-2 (gk257)* EGCG**	33.1 ± 0.4	27.5 ± 0.4	3	0.9525	788
***ctl-2 (ok1137)* DMSO**	32.5 ± 0.4	26.8 ± 0.7	3		602
***ctl-2 (ok1137)* ECG**	32.9 ± 0.5	27.2 ± 0.4	3	0.1718	614

Complex I inhibition by EGCG and ECG hampers mitochondrial respiration temporarily and induces a transient ROS signal

Previous reports have suggested that green tea catechins induce SIRT1/SIR-2.1 and FOXO/DAF-16 signaling by an initial increase in ROS levels. However, the ROS source has remained unidentified in previous reports [11]. We could confirm that ROS is essential for lifespan extension provoked by catechins, showing that the antioxidant butylated hydroxyanisole (BHA) prevents the life-prolonging effect of ECGC (Figure 2A) and ECG (Figure 2B). Moreover, we found that 25 µM of EGCG and ECG significantly hamper the activity of complex I in murine liver mitochondria (Figure 2C) and the mitochondrial respiration in mitochondria isolated from rat liver (Figure 2D). These findings are in line with reduced mitochondrial respiration in *C. elegans*

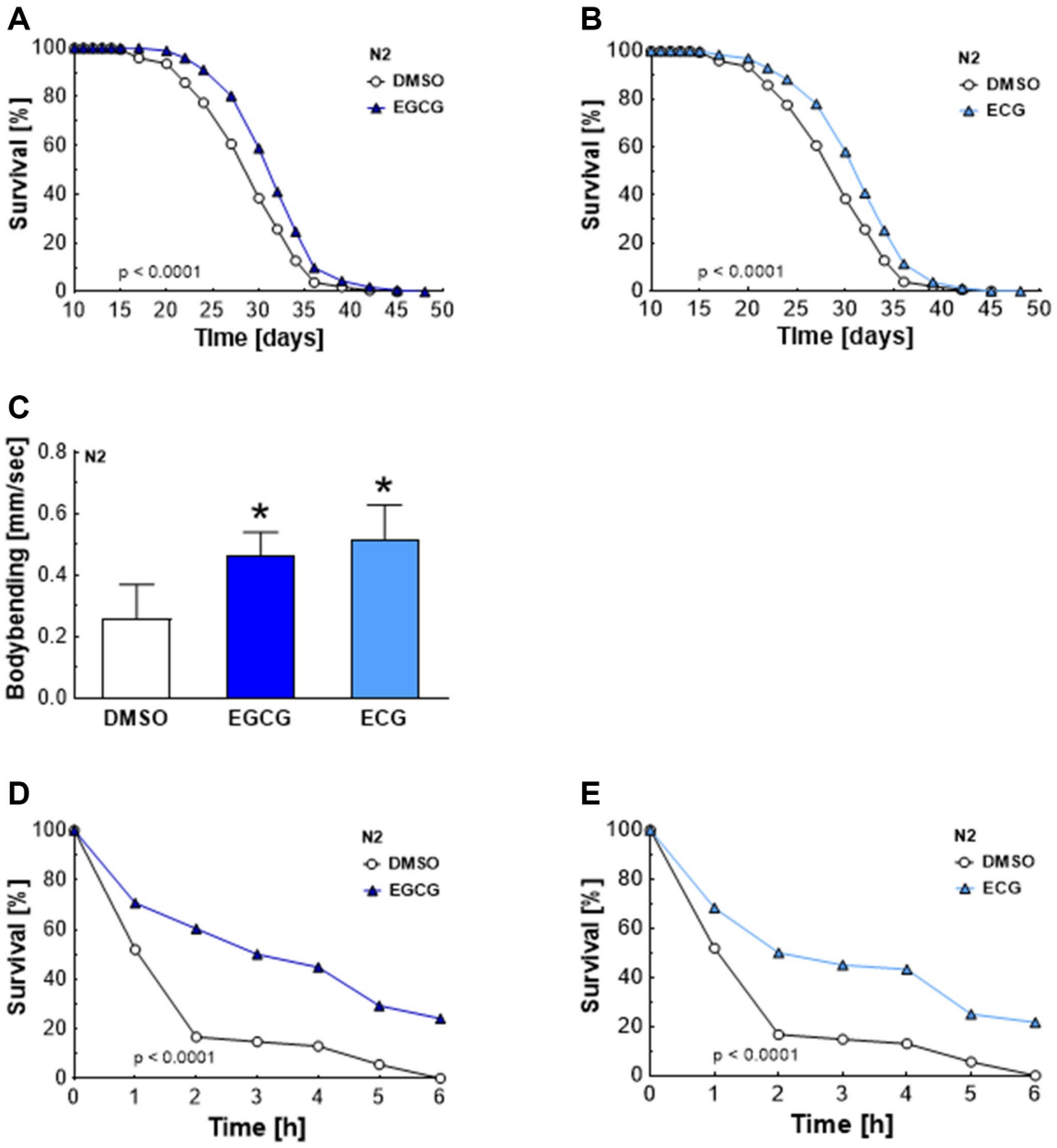

Figure 1. Increased lifespan, locomotion activity, and stress resistance after EGCG and ECG treatment. The representative outcome of lifespan assay of N2 wild-type nematodes in the presence of 2.5 µM EGCG versus DMSO. (**A**) The representative outcome of lifespan assay of N2 wild-type nematodes in the presence of 2.5 µM ECG versus control. (**B**) Locomotion quantification for N2 wild-type nematodes after 7 days exposure to DMSO, 2.5 µM EGCG, or 2.5 µM ECG. (**C**) The representative outcome of the survival analysis (h) of N2 nematodes in 50 mM paraquat solution after 7 days of pretreatment with EGCG (**D**) or ECG (**E**) in comparison to worms pretreated with DMSO. *P*-values are as indicated in the graphs. See Table 1 and Table 2 for corresponding detailed data and statistical analyses of lifespan assays and of paraquat stress assay, respectively.

Table 2. Paraquat stress assay results and statistical analysis.

Treatments	Number of experiments (*n*)	*P* value versus control	Number of nematodes
N2 DMSO	6		94
N2 EGCG	6	<0.0001	92
N2 ECG	6	<0.0001	93

after 6–12 hours exposure to 2.5 μM EGCG (Figure 2E) or ECG (Figure 2F). Notably, mitochondrial respiration recovered after 24 h and 120 h of treatment with EGCG (Figure 2E) and ECG (Figure 2F), pointing to compensation of an initially impaired mitochondrial function. The time course of initial diminution and the subsequent recovery of mitochondrial respiration correlates with ROS levels, which increased significantly after 6 h of ECGC (Figure 2G) and 12 h of ECG (Figure 2H) administration and dropped significantly after 24 h and 120 h of catechin treatment (Figure 2G, 2H).

AMPK and SIRT1 are essential for catechin-induced lifespan extension

Inhibition of complex I reduces NADH's oxidation to NAD+, necessary for glyceraldehyde 3-phosphate conversion to 1, 3-bisphosphoglycerate during glycolysis. Consequently, reduced levels of NAD+ hamper glycolysis and the production of pyruvate, which enters the Krebs cycle to be converted into water and CO_2 [16]. In line with these reports, ECGC reduced the oxidation of radioactively labeled glucose by 20%, as shown by impaired production of the ^{14}C-labeled CO_2 (Figure 3A). ECG treatment also tended to reduce the glucose turnover. However, the effects remained non-significant (Figure 3A). The time course of metabolic manipulation by EGCG and ECG was also reflected in overall ATP levels. In line with catechin-induced inhibition of mitochondrial respiration (Figure 2E, 2F) and glycolysis (Figure 3A), overall ATP levels dropped after 6 h of EGCG (Figure 3B) and 12 h of ECG (Figure 3C) treatment in nematodes before recovering after 24 h. A lack of ATP, resulting in a higher AMP to ATP ratio, is well-known to activate the AMP-dependent kinase AMPK [17]. The *C. elegans* homolog of AMPK, AAK-2, is involved in lifespan extension in response to impaired glycolysis [18] and insulin/IGF-1 signaling [19]. Indeed, EGCG (Figure 3D) and ECG (Figure 3E) failed to extend lifespan in *aak-2* deficient mutants. Notably, AMPK enhances NAD+-dependent type III deacetylase sirtuin 1 activity by increasing cellular NAD+ levels [20]. In *sir-2.1* defective mutants, EGCG (Figure 3F) and ECG (Figure 3G) did not achieve a lifespan extension, proving that EGCG and ECG prolong lifespan in an AMPK- and SIRT1-dependent manner. These findings align with previous reports showing that catechins' lifespan extension depends on AMPK, SIRT1, and FOXO [11].

p38 MAPK, NRF2, and FOXO are required for the lifespan extension induced by catechins

As shown in Figure 2, EGCG and ECG block complex I activity and, thus, induce a transient rise in ROS levels. ROS [21] and AMPK [22] are potential mediators of the p38 MAP kinase pathways. The homolog of the mammalian p38 MAPK, PMK-1, has been identified as a crucial component in the lifespan extension of *C. elegans* [23, 24]. In line with these previous reports, we found that neither EGCG (Figure 4A) nor ECG (Figure 4B) treatment extends lifespan in *pmk-1* deficient mutants. Next, we tested the impact of whether the transcription factor SKN1, the worm homolog of NRF2 and a downstream target of PMK1 under conditions of oxidative stress [25–27], is involved in the lifespan extension provoked by catechins. Again, no EGCG- (Figure 4C) or ECG-induced (Figure 4D) lifespan extension could be observed in *skn-1* mutant worms. DAF-16 is the homolog of a mammalian FOXO and is reported to respond to physical and environmental stress [28]. *daf-16* mutant worms are sensitive to oxidative stress and have shortened lifespans. Moreover, DAF-16 can activate or repress the transcription of target genes involved in dauer formation, life span, stress resistance, and fat storage of *C. elegans* [29]. EGCG and ECG decreased mean lifespan in *daf-16* deficient nematodes from 20.1 ± 0.1 to 19.8 days (Figure 4E) and from 20.1 ± 0.1 to 19.4 ± 0.2 days (Figure 4F), respectively. The maximum lifespan was decreased from 22.5 ± 0.3 to 22.2 ± 0.2 days by EGCG treatment (Figure 4E) and from 22.5 ± 0.3 to 21.7 ± 0.6 days by ECG treatment (Figure 4F). These results suggest that DAF-16 is indispensable for EGCG's and ECG's lifespan extension and show that *daf-16* deficient nematodes are especially prone to a ROS level rise induced by catechins.

EGCG and ECG induce adaptive responses in ROS homeostasis and cellular metabolism

AMPK/SIRT1 and p38MAPK/NRF2/FOXO signaling cascades are associated with antioxidant defense mechanisms [30]. The major antioxidant enzymes in *C. elegans* include five distinct superoxide dismutases, converting superoxide to hydrogen peroxide, and two catalases, which ensure the subsequent conversion of hydrogen peroxide to water [31]. EGCG treatments increased SOD activity after 24 h (Figure 5A) and CTL activity after 7 days (Figure 5B). Meanwhile, ECG

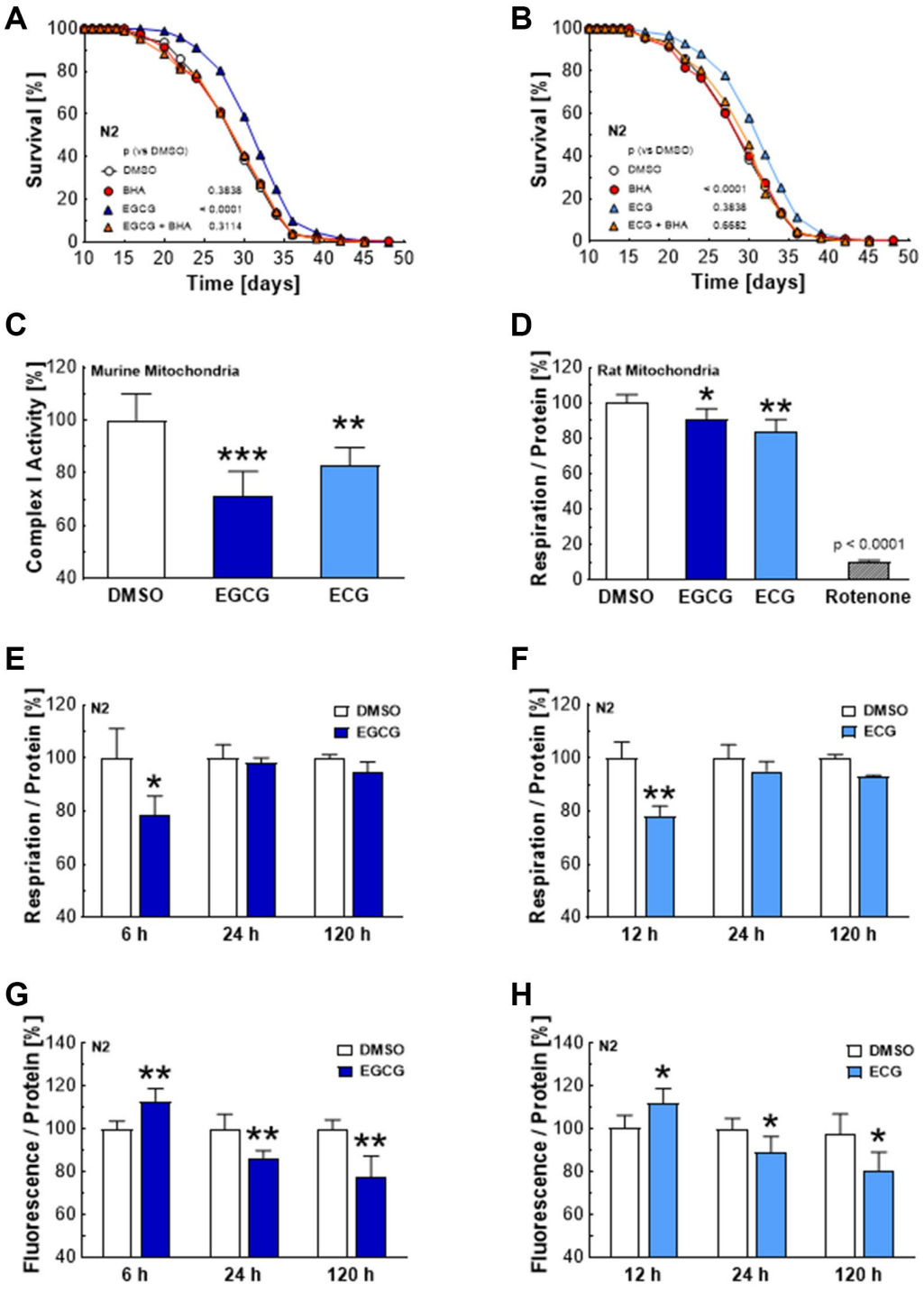

Figure 2. EGCG and ECG inhibit complex I, which results in a temporary hampering of mitochondrial respiration and a boost in ROS production. The representative outcome of lifespan assay of N2 wild type nematodes in the presence of 2.5 µM EGCG co-applied with an antioxidant; DMSO vs. 2.5 µM EGCG vs. 10 µM BHA vs. 2.5 µM EGCG in combination with 10 µM BHA. (**A**) The representative outcome of lifespan assay of N2 wild type nematodes in the presence of 2.5 µM ECG co-applied with an antioxidant; DMSO vs. 2.5 µM ECG vs. 10 µM BHA vs. 2.5 µM ECG in combination with 10 µM BHA. (**B**) Complex I activity in murine liver mitochondria after treatment with DMSO, 25 µM EGCG or 25 µM ECG. (**C**) Mitochondrial respiration of rat liver mitochondria after treatment with DMSO, 25 µM EGCG or 25 µM ECG. (**D**) Mitochondrial respiration of N2 wild-type nematodes after treatment with DMSO or 2.5 µM EGCG for 6 h, 24 h, or 120 h measured as oxygen consumption rate and normalized to protein content. (**E**) Mitochondrial respiration of N2 wild-type nematodes after treatment with DMSO or 2.5 µM ECG for 12 h, 24 h, or 120 h, measured as oxygen consumption rate and normalized to protein content. (**F**) ROS production of N2 wild-type nematodes after treatment for 6 h, 24 h, or 120 h with 0.1% DMSO or 2.5 µM EGCG. (**G**) ROS production of N2 wild-type nematodes after treatment for 6 h, 24 h, or 120 h with 0.1% DMSO or 2.5 µM ECG. (**H**) *P*-values are as indicated in the graphs. See Table 1 for corresponding detailed data and statistical analyses of lifespan assays.

treatments did not significantly increase SOD activity (Figure 5A) but increased CTL activity after 24 h and 7 days (Figure 5B). The enhanced activity of SOD and CTL correlates with the subsequent drop of ROS levels after 24 h of EGCG and ECG treatment. Notably, the lifespan-extending effect of EGCG and ECG is dependent on SOD-2 (Figure 5C) and catalase 2 (CTL-2) (Figure 5D). As shown in Figure 3, complex I inhibition by EGCG and ECG was also accompanied by a reduction in glucose oxidation. In line with this

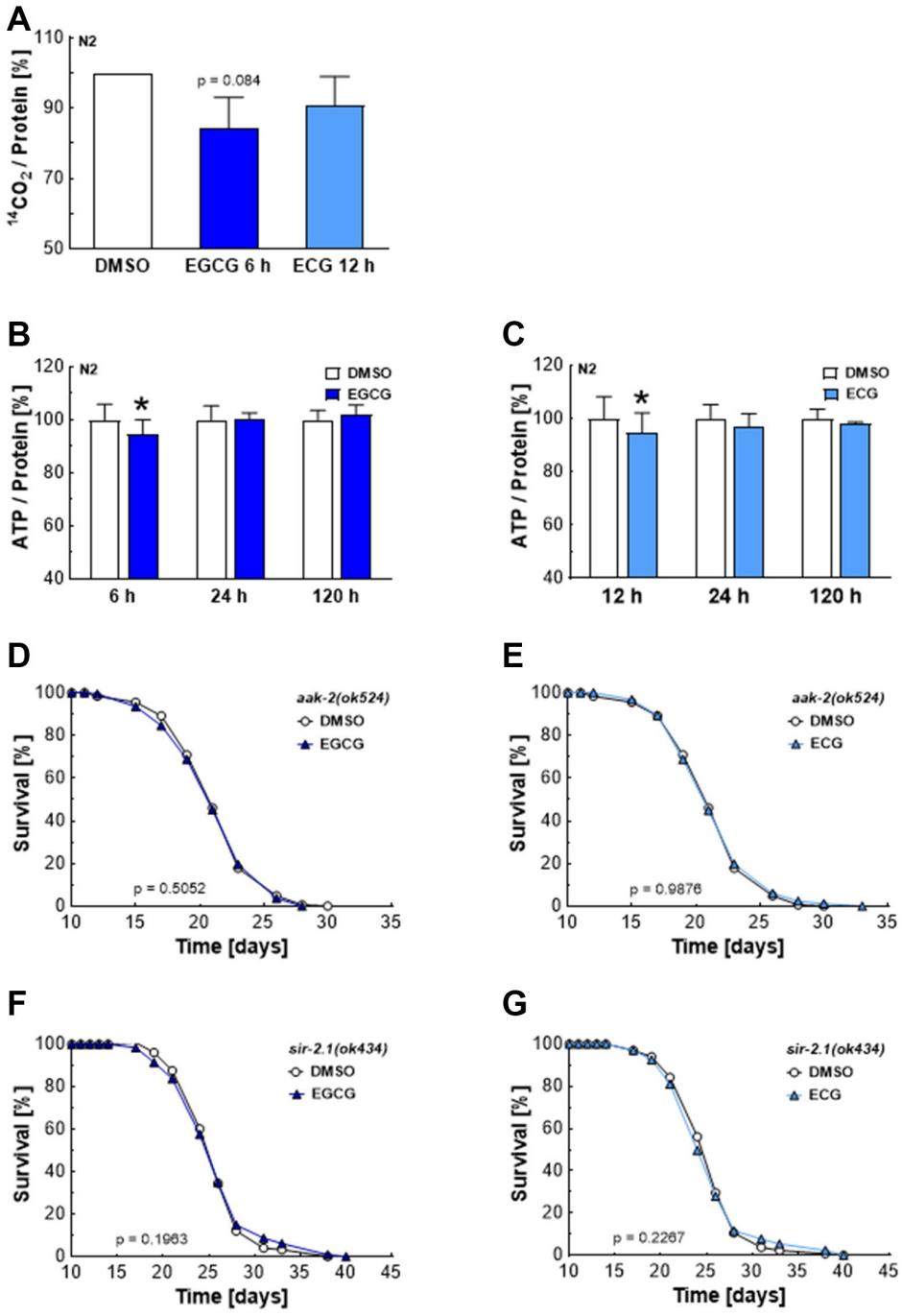

Figure 3. EGCG and ECG induce a drop in cellular ATP levels and require AMPK/SIRT1 signaling to extend lifespan. $^{14}CO_2$ production of N2 wild-type nematodes after treatment with 0.1% DMSO, 2.5 µM EGCG or 2.5 µM ECG for the indicated time. (**A**) ATP content for various incubation periods of N2 wild-type nematodes with 0.1% DMSO or 2.5 µM EGCG. (**B**) ATP content for different incubation periods of N2 wild-type nematodes with 0.1% DMSO or 2.5 µM EGCG. (**C**) The representative outcome of lifespan assay of *aak-2* mutants treated with 0.1% DMSO versus 2.5 µM EGCG (**D**) or 2.5 µM ECG. (**E**) The representative outcome of lifespan assay of *sir-2.1* mutants treated with 0.1% DMSO versus 2.5 µM EGCG (**F**) or 2.5 µM ECG. (**G**) *P*-values are as indicated in the graphs. See Table 1 for corresponding detailed data and statistical analyses of lifespan assays.

finding, the fat content was found to be significantly lower after 120 h of EGCG or ECG treatment (Figure 5E), pointing to a catechin-induced long-term reprogramming of cellular metabolism.

DISCUSSION

Green tea is one of the most widely consumed beverages worldwide [32]. The popularity of green tea makes it crucial to study its impact on health and aging. Although EGCG's and ECG's bioavailability is relatively low [7, 8], consuming 4 cups of green tea daily for 8 weeks significantly decreases body weight [33]. Previous reports already reported a lifespan extension in *C. elegans* after treatment with 50–300 µM EGCG [11]. Here, we show that already 2.5 µM of EGCG and ECG, a concentration also potentially achieved after green tea consumption [14], are sufficient

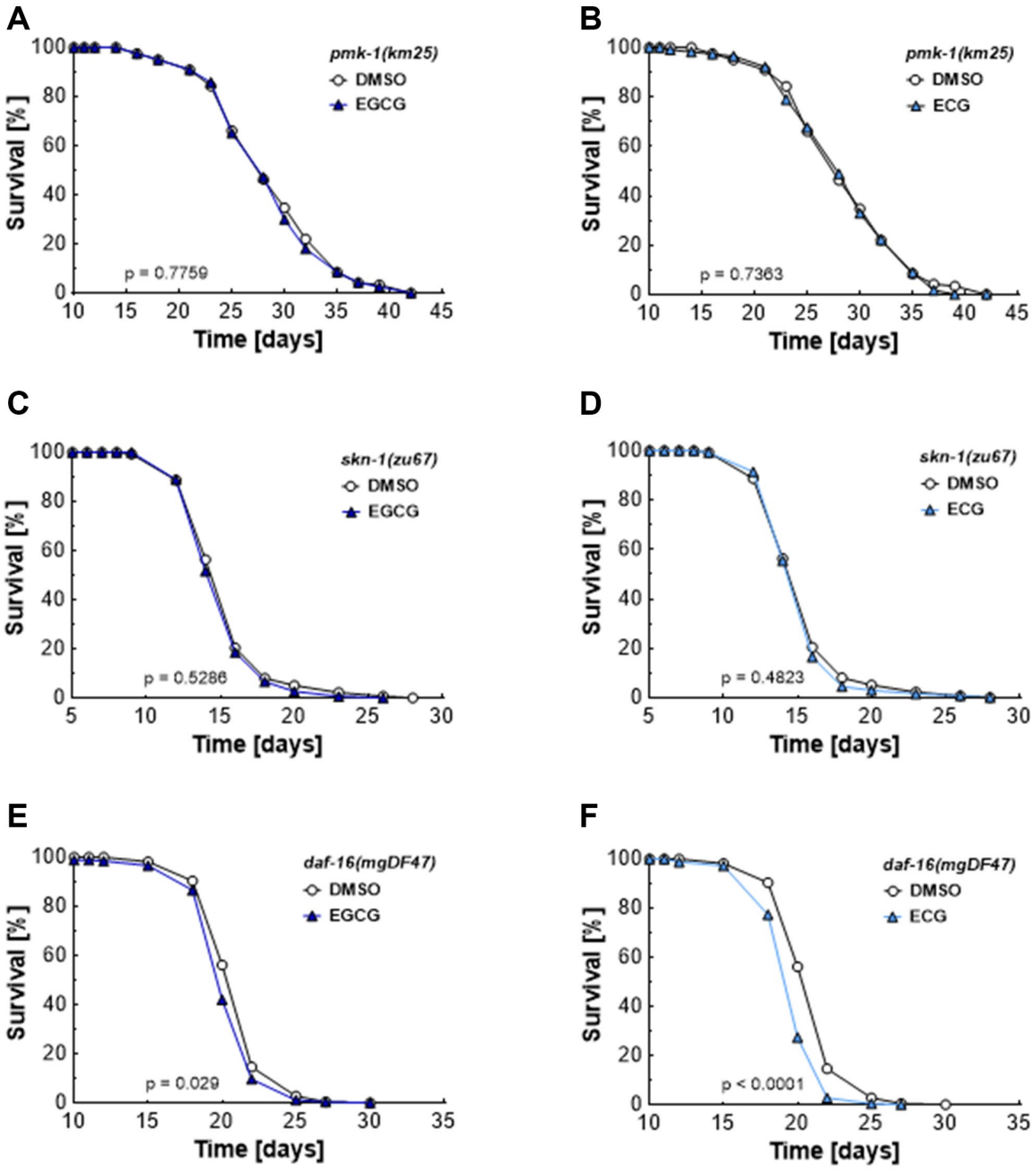

Figure 4. EGCG and ECG mediate lifespan extension dependent on PMK-1/p38 MAPK, SKN-1/NRF2, and DAF-16/FOXO. The representative outcome of lifespan assay of *pmk-1* mutants treated with 0.1% DMSO versus 2.5 µM EGCG (**A**) or 2.5 µM ECG. (**B**) The representative outcome of lifespan assay of *skn-1* mutants treated with 0.1% DMSO versus 2.5 µM EGCG (**C**) or 2.5 µM ECG. (**D**) The representative outcome of lifespan assay of *daf-16* mutants treated with 0.1% DMSO versus 2.5 µM EGCG (**E**) or 2.5 µM ECG. (**F**) *P*-values are as indicated in the graphs. See Table 1 for corresponding detailed data and statistical analyses of lifespan assays.

to induce an extension of lifespan and increase stress resistance by adaptational mechanisms. In this mitohormetic response, EGCG and ECG act initially as prooxidants by provoking a ROS rise. Since a transient ROS burst induces antioxidant defense mechanisms, EGCG and ECG display antioxidant properties in the long term. In higher concentrations, EGCG and ECG might show harmful effects due to excessive ROS production. This phenomenon gets obvious in studies performed on cancer cells. While the antioxidant potential of green tea catechins in low concentrations was suggested as a potential solution to prevent tumorigenesis [34, 35], higher dosages of catechins might serve as antitumor agents due to the induction of overwhelming ROS formation and apoptosis [36–41]. Notably, EGCG was more potent than ECG in human cancer cell lines in inducing cytotoxic effects [33] and inhibiting cancer cell motility [42]. Indeed, it took just 6 h for EGCG, but 12 h

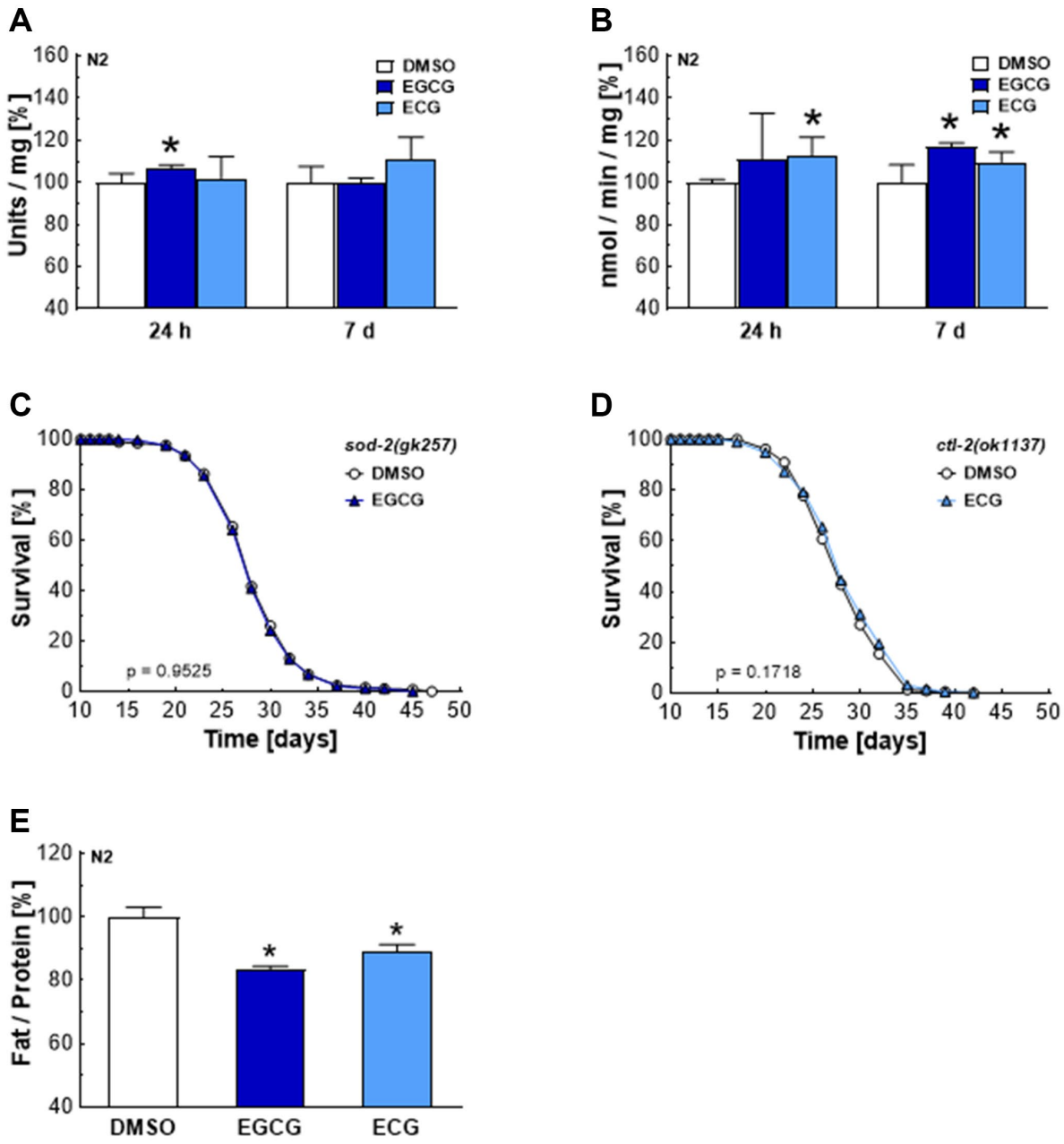

Figure 5. EGCG and ECG induce SOD and CTL activity and a shift in lipid metabolism in the long term. SOD (**A**) or CTL (**B**) activity after treatment with 0.1% DMSO, 2.5 µM EGCG or 2.5 µM ECG for 24 h or 7 days. The representative outcome of lifespan assay of *sod-2* mutants treated with 0.1% DMSO or 2.5 µM EGCG. (**C**) The representative outcome of lifespan assay of *ctl-2* mutants treated with 0.1% DMSO or 2.5 µM ECG. (**D**) Triglyceride content in N2 wild-type nematodes after treatment with 0.1% DMSO, 2.5 µM EGCG or 2.5 µM ECG for 5 days, normalized to protein content. (**E**) *P*-values are as indicated in the graphs. See Table 1 for corresponding detailed data and statistical analyses of lifespan assays.

for ECG to affect mitochondrial respiration, ROS, and ATP levels. However, the impact of these compounds was similar when applied in the long term, yielding similar effects on lifespan, motility, and stress resistance.

Besides triggering a mitohormetic response through their effects on transcription factors and enzyme activities, catechins were speculated to exert direct antioxidant potential by scavenging ROS [43, 44]. While a modest increase in the plasma antioxidant capacity following green tea consumption was reported [43], the fraction of structurally intact catechins reaching target tissues is insignificant compared to the antioxidant potential due to intracellular glutathione achieving levels of 1–11 mM [45–47]. Besides, EGCG even induced hydrogen peroxide formation in the cell culture and liquid NGM system [44–46]. Moreover, hydrogen peroxide mimicked the effect of EGCG on signaling pathways, while antioxidants abolished the impact of catechins [37, 41, 48–50]. We could show that BHA prevented lifespan extension by EGCG and ECG, suggesting that an initial rise in ROS levels is necessary to induce adaptational mechanisms causing improved antioxidant properties.

Previous studies already revealed increased hydrogen peroxide levels and a dose- and time-dependent decrease in glutathione levels in cell culture models after applying 50 µM of EGCG [43, 51]. However, the mechanism of how EGCG and ECG induce ROS formation was not described so far [11]. In the current study, we revealed that EGCG and ECG inhibit complex I of the ETC. Experiments in rat cerebellar granule neurons have shown that EGCG accumulates explicitly in mitochondria, reaching 90–95% mitochondrial accumulation of this polyphenol [52]. This finding is well aligned with the plethora of literature describing polyphenols as compounds targeting mitochondria [53, 54]. Consequently, we isolated mitochondria to investigate the impact of EGCG and ECG on the complexes of the mitochondrial ETC. Isolated mitochondria are separated from their natural environment and signaling processes, and the isolation process brings the risk of damaging mitochondrial membranes due to shear forces [55]. However, drug uptake by mitochondria is dependent on the integrity of the outer and inner mitochondrial membrane, including the function of transporter proteins and carriers [56]. Since 25 µM of EGCG and ECG were necessary to achieve a significant inhibition of complex I activity in mitochondria isolated from murine liver samples and to hamper mitochondrial respiration in mitochondria isolated from rat liver, we assume that the isolation process affected the integrity of mitochondrial membranes and, thereby, mitochondria's potential to take up catechins efficiently. Besides, the isolation of mitochondria yields a relatively homogenous population of spherical organelles with disorganized cristae and diluted matrix content. The structural alterations affect ETC activity and mitochondrial respiration rate [57]. We assume that structural changes in cristae organization due to the isolation process might be another reason why 25 µM of EGCG and ECG were necessary to significantly block complex I activity and mitochondrial respiration rate in isolated mitochondria.

In addition, we present that a temporary hampered mitochondrial respiration goes along with a transient rise in ROS levels and a brief drop in ATP, triggering signaling pathways associated with lifespan extension in *C. elegans*. Our findings align with reports about the *C. elegans* mutant *nuo-6(qm200)*, carrying a mutation in a conserved subunit of mitochondrial complex I (NUDF84). This specific mutant has reduced complex I function, increased ROS levels [58], and a prolonged lifespan [59]. It was also speculated that blockage of the complex I of the mitochondrial electron transport chain delays aging due to slowed embryonic development and larval growth, decreased pumping and defecation rate, or a reduced accumulation of ROS damage [60–62]. However, RNAi-induced knockdown of the mitochondrial electron transport chain's complexes at the L3/L4 stage is sufficient to initiate lifespan extension in *C. elegans*. At this stage, mitochondria are already undergoing a period of dramatic proliferation and massive mitochondrial DNA expansion [63]. Moreover, inhibiting respiratory chain components during adulthood did not provoke lifespan extension anymore [64–66]. Consequently, one has to assume that a temporary sub-lethal rise in mitochondrial ROS during early adulthood induces lifespan extension by provoking changes in the homeostasis of proteins [59, 67] and metabolism [58]. Notably, glucose restriction by 2-deoxy-D-glucose (2-DG)-mediated inhibition of glycolysis increases the lifespan in *C. elegans* in a ROS-dependent manner [18], suggesting that the temporary drop in ATP levels due to complex I inhibition is an additional trigger to prolong lifespan.

Our data demonstrate that life span extension by EGCG and ECG involves energy sensors AAK-2/AMPK and SIR-2.1/SIRT1 as well as the ROS-sensing PMK-1/p38 MAPK, and the transcription factors SKN-1/NRF2 and DAF-16/FOXO. By activating these signaling cascades, the function of ROS defense enzymes, SOD and CTL, and the oxidative stress resistance gets boosted. A previous report presented that catechins' lifespan extension depends on AMPK, SIRT1, and FOXO [11]. Ahead of this report, SOD-3, DAF-16, and SKN-1 were already suggested as targets of EGCG due to enhanced expression [68] or translocation into the nucleus after respective compound treatment [48]. Oxidative stress was reported to stimulate SKN-1's translocation to the

nucleus, a process tightly regulated by protein kinases, including PMK-1, GSK-3, MKK-4, IKK epsilon-1, NEKL-2, and PDHK-2 [26]. Notably, SKN-1 activation in neurons is necessary for dietary restriction-mediated lifespan extension [69]. Moreover, reduced insulin/IGF-1 signaling causes nuclear accumulation of SKN-1, a process needed for long-lived *daf-2* mutants with increased stress resistance and lifespan [19, 70]. DAF-16, the orthologue of mammalian FOXO, is a crucial regulator of longevity, metabolism, and dauer diapauses in *C. elegans* [28, 29, 71, 72]. Consequently, it seems reasonable that the ROS-sensing p38 MAPK and the energy-sensing AMPK activate the respective signaling cascades after blockage of complex I by EGCG and ECG. Reports showed that AMPK activates p38 MAPK [73]. Consequently, these two kinases might even augment each other's activity and the potential of the respective signaling cascade.

The long-term effects also included reduced fat content in *C. elegans* after 5 days of catechin treatment. Align with this finding, inhibition of complex I and complex IV by rotenone and NaN3 reduced lipid accumulation in 3T3-L1 cells [74]. Moreover, a previous report revealed reduced body fat content in *C. elegans* after catechin treatment [75]. Besides, green tea catechins were associated with reduced obesity in zebrafish [76], mice [77], rats [78, 79], and humans [80, 81], suggesting a catechin-induced metabolic remodeling.

Clinical trials have already confirmed the safety of EGCG [7] and highlighted the potential in counteracting age-related cardiovascular and metabolic diseases [1–4]. Experiments in rodents studying physical and clinical parameters over time and further clinical trials are required to identify the best timing and dosage for administering catechins. Finally, these studies might characterize additional effects and downstream mechanisms of complex I inhibition. Despite the promising results obtained in animal experiments, the low bioavailability of EGCG [7] still raises the question of whether green tea catechins can reliably provoke beneficial effects in humans. Consequently, additional efforts might be needed to identify complex I inhibitors with increased bioavailability.

CONCLUSIONS

We conclude that applying the green tea catechins EGCG and ECG at a low dose extends the lifespan of *C. elegans* via inducing a mitohormetic response. Thereby, the inhibition of complex I causes a transient ROS rise that stimulates the antioxidant defense enzymes SOD and CAT and activates the PMK-1/SKN-1/DAF-16 pathway (Figure 6, Scheme). Besides, complex I inhibition causes a temporary drop in cellular ATP levels and consequently activation of AAK-2/SIR-2.1 signaling. In the long term, the re-wiring of these energy- and ROS-dependent pathways reduces the fat content and extends health- and lifespan.

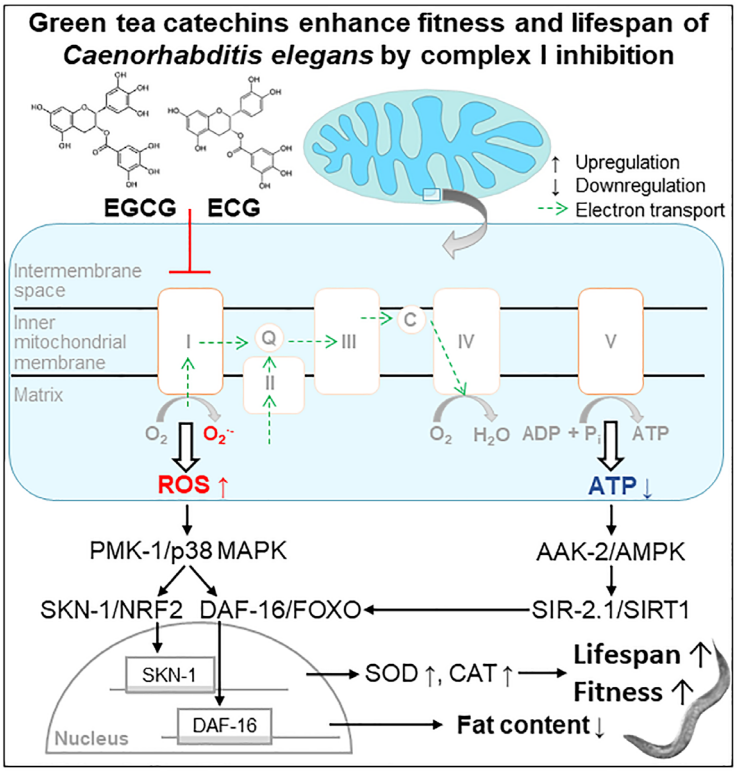

Figure 6. Scheme. Green tea catechins enhance fitness and lifespan of *Caenorhabditis elegance* by complex I inhibition.

METHODS

Nematode strains and maintenance

C. elegans strains used in the current study were obtained from the *Caenorhabditis* Genetics Center (CGC, University of Minnesota). Nematodes were grown and maintained at 20°C in 10 cm Petri dishes on nematode growth media (NGM), with *Escherichia coli (E. coli)* OP50 bacteria as the food resource as previously described [18, 82, 83]. The strains used in this study included the following: N2 (wild type), GA1001 *aak-2(ok524)*, VC199 *sir-2.1(ok434),* KU25 *pmk-1(km25)*, EU1 *skn-1(zu67),* IU10 *daf-16(mgDF47),* GA184 *sod-2(ok257)*, and VC754 *ctrl-2(ok1137).*

Compound treatment

EGCG, ECG, and BHA dissolved in DMSO, reaching a stock concentration of 2.5 mM of EGCG and ECG and 10 mM of BHA. The NGM agar solution was autoclaved and subsequently cooled to 55°C, before supplements and compounds (EGCG, ECG, BHA, or DMSO) were added under continuous stirring. The final concentration for compounds was calculated regarding the volume of agar, and the same volume of DMSO was added to control plates. NGM agar plates were supplemented with 100 µg/ml ampicillin to induce metabolic inactivity in *E. coli*. Agar plates were poured and dried, sealed with parafilm, and stored at 4°C. Before experiments, NGM plates were spotted with a bacterial lawn of heat-inactivated bacteria (OP50 HIT) to avoid interference by a potential xenobiotic-metabolizing activity of *E. coli*. To exclude any effects on development, the incubation period with compounds started at the L4 stage by transferring nematodes to the respective NGM plates [84]. To analyze oxygen consumption rate, glucose oxidation, ATP levels, enzyme activity, and fat content, adult worms at the L4 stage were transferred on NGM agar plates containing 25 µM 5-fluoro-2′-deoxyuridine (Sigma-Aldrich, St. Louis, MO, USA) to prevent progeny formation. After 16 h, we transferred animals to respective treatment groups and harvested them at the indicated time points [18].

Lifespan analyses

According to standard protocols, all lifespan assays were performed at 20°C as previously described [18, 19]. Briefly, the *C. elegans* population was synchronized with hypochlorite/NaOH solution except for *skn-1* mutant worms. Eggs from heterozygous *skn-1* hermaphrodites were harvested after overnight egg-laying without applying hypochlorite/NaOH solution to increase the yield of viable larvae [85]. Eggs of nematodes were transferred to NGM plates with fresh OP50 bacteria to allow hatching and development. After approximately 64 h, at the L4 stage, we moved 200 nematodes manually to freshly prepared NGM plates containing the respective compounds and supplied them with a lawn of OP50 HIT. During the first 10–14 days, nematodes were transferred to freshly prepared NGM treatment plates every day and later every second day. Nematodes without any reaction to gentle stimulation were classified as dead. Nematodes that crawled off the plate or suffered from non-natural death like internal hatching were censored and excluded from statistics on the day of premature death. Notably, for lifespan analysis using BHA, nematodes were propagated on BHA-containing NGM plates for four generations before synchronization; the same applied for the respective DMSO controls.

Locomotion assay

Following the L4 stage, nematodes were treated with 0.1% DMSO, 2.5 µM of EGCG, and 2.5 µM of ECG for 7 days. Afterward, we transferred single worms into S-buffer containing 0.01% Triton X-100 to wash off bacteria and then pipetted them on a glass slide. Movements of single worms within the liquid system were recorded for 20 seconds by a digital CCD camera (Moticam 2300, Motic, St. Ingbert, Germany) coupled microscope (SMZ 168, Motic, St. Ingbert, Germany) equipped with Motic Images Plus 2. We analyzed the videos using the DanioTrack software (Loligo Systems, Tjele, Denmark), subtracting the background and determining the center of gravity of all object pixels compared to the background. As described previously, the center's shift distance was accumulatively calculated and normalized per second [84].

Paraquat stress resistance assay

Resistance to lethal oxidative stress by paraquat (Sigma-Aldrich, Munich, Germany) was assessed as previously described [18, 19]. Briefly, worms were treated with 0.1% DMSO, 2.5 µM of EGCG, and 2.5 µM of ECG for 7 days after L4 stage. Afterward, we transferred worms into 96-well plates: 6 nematodes in 100 µl of S-buffer, containing freshly dissolved 50 mM paraquat. Dead worms were scored every hour until all control worms were dead.

Basal oxygen consumption rate

Mitochondrial respiration was quantified using a DW1/AD Clark-type electrode (Hansatech, King's Lynn, England) as previously described [18]. Briefly, we treated worms with 0.1% DMSO, 2.5 µM EGCG, or 2.5 µM ECG for the indicated periods, then washed off the

respective NGM plates with S-buffer and allowed them to settle by gravitation to remove offspring and bacteria. Worms were also washed twice with S-buffer and transferred into the DW1 chamber to monitor oxygen consumption for 10 mins. Afterward, we collected worms for Bradford protein determination [86].

ROS quantification

Before the ROS measurement, MitoTracker Red CM-H2X ROS (Invitrogen, Carlsbad, CA, USA) incubation plates were prepared as previously described [19]. Briefly, we treated worms with 0.1% DMSO, 2.5 µM EGCG, or 2.5 µM ECG for the indicated periods, then washed off the respective NGM plates and allowed them to settle by gravitation to remove offspring and bacteria. Worms were additionally washed twice with S-buffer and transferred to freshly prepared MitoTracker Red CM-H2X incubation NGM plates containing 500 µl of OP50 HIT mixed with 100 µl freshly prepared MitoTracker Red CM-H2X stock solution (100 µM). After 2 h at 20°C, worms were washed off MitoTracker Red CM-H2X incubation NGM plates and transferred to NGM agar plates with 0.1% DMSO, 2.5 µM EGCG or 2.5 µM ECG for 1 h to remove excess dye from the gut. Aliquots of 100 µl worm suspension in S-buffer were distributed into a 96-well FLUOTRAC™ plate (Greiner Bio-One, Frickenhausen, Germany). Fluorescence intensity was measured on a microplate reader (FLUOstar Optima, BMG Labtech, Offenburg, Germany) using well-scanning mode (ex: 570 nm; em: 610 nm). We collected worms from plates for Bradford protein determination [86].

Glucose oxidation assay

[^{14}C] D-glucose oxidation rates were determined as described previously [87]. Uniformly labeled [^{14}C] D-glucose was purchased from PerkinElmer, and the specific activity of the batch used was 300 mCi/mmol. We placed an equal number of nematodes on the NGM plates containing 0.1% DMSO, 2.5 µM EGCG, or 2.5 µM ECG for the indicated period. After collection and two subsequent washes in S-buffer, worm pellets were resuspended in the incubation buffer. 700 µl of the suspension were transferred to 4 cm Petri dishes. The latter were placed in 10 cm Petri dishes together with a second 4 cm Petri dish containing 600 µl of 0.1 M KOH solution to trap CO_2 as described previously [18, 88]. Hence, each 10 cm dish was equipped with two 4 cm dishes, one carrying nematodes and the other containing KOH. We added labeled glucose to a final concentration of 17 µM U-[14C] D-glucose (5 µCi/ml) in the nematode suspension as a substrate. We added nonradioactive glucose into each sample to reach a final concentration of 0.5 mM. The 10 cm Petri dishes were covered, sealed with parafilm in an air-tight manner, and incubated at 20°C for 3 h. Subsequently, an aliquot of 500 µl of KOH was immersed in 4.5 ml of scintillation fluid and placed in a liquid scintillation counter (Beckmann LS 6000, Global Medical Instrumentation, Inc.) to quantify the amount of trapped $^{14}CO_2$. We normalized $^{14}CO_2$ signals to incubated worms' protein content.

ATP quantification

We treated nematodes with 0.1% DMSO, 2.5 µM EGCG, or 2.5 µM ECG for the indicated time. After collection and washing with S-buffer twice, worm pellets were shock frozen in liquid nitrogen and grinded in a nitrogen-chilled mortar. The grinded samples were boiled with 4 M Guanidine-HCl at 99°C for 15 min to destroy ATPase activity [58, 89]. Precipitated proteins were separated by centrifugation (30 min, 13200 g at 4°C), and the supernatant was analyzed regarding the ATP content using CellTiter Glo (Promega, Fitchburg, WI, USA) according to the manufacturer's instructions. ATP values were normalized to protein content using the Bradford assay [86].

Activity assays for Catalase (CTL) and Superoxide Dismutase (SOD)

After treating nematodes with 0.1% DMSO, 2.5 µM EGCG, or 2.5 µM ECG for the indicated period, the respective enzyme activities were determined by standard photometric assays as previously described [18, 19, 84]. Briefly, CTL activity was estimated by the production of formaldehyde due to the enzyme's reaction with methanol in the presence of an optimal concentration of H_2O_2. The produced formaldehyde was determined spectrophotometrically with 4-amino-3-hydrazino-5-mercapto-1, 2, 4-triazole (Purpald, Applichem, Darmstadt, Germany). We measured SOD activity photometrically with a tetrazolium salt, forming a water-soluble formazan dye upon reduction with a superoxide anion.

Fat content analysis

We determined fat content by applying a triglyceride determination kit (Roche, Mannheim, Germany) as previously described [18, 88] and normalized to protein content using the Bradford assay [86]. Briefly, worms were incubated with 0.1% DMSO, 2.5 µM EGCG, or 2.5 µM ECG for 5 days, washed, and shock-frozen in liquid nitrogen. Afterward, worm pellets were grinded in a nitrogen-chilled mortar with Milli-Q water supplemented with 5% Triton X-100 and sonicated 3 times. We centrifuged 200 µl of the homogenized

extract and extracted the supernatant for protein determination. 400 µl of lysate was heated to 80°C for 5 min and then cooled down to room temperature. The heating was repeated once to dissolve all triglycerides. After heating and cooling, the lysate was centrifugated at 12000 *g* for 10 min, and we collected the supernatant for triglyceride determination according to the manufacturer's protocol.

Quantification of complex I activity in mitochondria from the murine liver

We measured the activity of complex I spectrophotometrically at 600 nm in 1 ml of 25 mM potassium phosphate buffer containing 3.5 g/L BSA, 60 µM 2,6-dichloroindophenol (DCIP), 70 µM decylubiquinone, 1.0 µM antimycin A, and 0.2 mM NADH, adjusted to pH 7.8 [90]. Decylubiquinone and antimycin A were dissolved in DMSO as 17.5 mM and 1.0 mM, respectively. DCIP and NADH were dissolved in water as 10 mM for both. BSA stock solution was 70 g/L in 5 mM potassium phosphate buffer, pH 7.4. Mouse liver mitochondria stocks contained 10 µg/µl in 10 mM Tris (pH 7.6) and were stored at −80°C. After being thawed, 30 µl of mitochondria were treated with 470 µl of 10 mM Tris-Cl, pH 7.6, to disrupt the mitochondrial membrane. Subsequently, 20 µl mitochondria fragments were preincubated in a 960 µl incubation mixture without NADH for 3 mins. After 3 mins, we added 20 µl of 10 mM NADH into the incubation mixture and measured the absorbance at 20 s intervals for 2 mins. 2 mins later, 1 µl of DMSO, EGCG, or ECG were added into the incubation mixture as fast as possible and measured absorbance again at 20s intervals for 4 mins. The effect of chemicals on complex I activity was expressed as the slopes' ratio of decreasing absorbances before and after adding substances.

Isolation of mitochondria from murine liver

We did the isolation of mitochondria from rat liver according to Frezza's protocol [91], except for the homogenization, which was done using a tissue glass Dounce Homogenizer (Wheaton, VWR, Darmstadt, Germany). Briefly, rodents were fasted overnight and killed by cervical dislocation. The liver was rapidly explanted, immersed, and sliced in the isolation buffer containing 200 mM sucrose, 1 mM EGTA/Tris, and 10 mM Tris/MOPS, pH 7.4. The washed liver fragments were placed into the tube with around 25 ml isolation buffer. The loose-fitting pestle was inserted, pressed down, and lifted four times, and then the tight-fitting pestle was applied in the same way twice. The mixture was poured into the 50 ml polypropylene falcon tube and centrifuged at 600 *g* for 10 min at 4°C. We carefully removed the fat on the top of the supernatant by using tissue paper. The supernatant was extracted to a second polypropylene falcon tube centrifuged at 7000 *g* for 10 min at 4°C. Afterward, the fat was removed, the supernatant discarded, and the mitochondrial pellet resuspended in the remaining buffer. The suspension containing mitochondria was centrifuged again at 7000 *g* for 10 min at 4°C. The supernatant was removed entirely, and the mitochondrial pellet was resuspended in 200 µl isolation buffer as described above. The concentration of isolated mitochondria was determined with Bradford (1976).

Quantification of oxygen consumption rate in murine liver mitochondria

Mitochondria respiration was quantified using a DW1/AD Clark-type electrode (Hansatech, King's Lynn, England) at 30°C in 1 ml experiment buffer containing 125 mM KCl, 10 mM Tris/MOPS, 0.1 mM EGTA/Tris and 1 mM KH_2PO_4, pH 7.4, as previously described [91]. 5 mM Glutamate and 2.5 mM Malate were supplied as substrates for complex I, III, IV. After recording basal respiration for 2 min, 0.1% DMSO, 25 µM EGCG, or 25 µM ECG and subsequently 100 µM ADP was added. After ADP was wholly consumed, the oxygen consumption rate slowed down, 5 mM succinate, and ADP were added to study complex II, III, IV activity. At the end of each measurement 60 nM FCCP were supplied to check the viability of mitochondria.

Statistical analyses

Data are expressed as means ±SD unless otherwise indicated. Statistical analyses for all data except lifespan assays and stress resistance assays were performed by Student's *t*-test after testing for equal distribution of the data and equal variances within the data set. Statistical calculations were carried out using the log-rank test to compare significant distributions between the different groups in lifespan and stress resistance assays. We performed all analyses using Microsoft Office Excel 2016 (Microsoft, Albuquerque, NM, USA). Differences were considered statistically significant at $p < 0.05$ and presented as specific *p*-values ($^{*}p \leq 0.05$; $^{**}p \leq 0.01$; $^{***}p \leq 0.001$).

AUTHOR CONTRIBUTIONS

J.T., C.G., and C.T.M. performed experiments, analyzed, and visualized the data. C.T.M. and M.R. wrote the manuscript. Funding was acquired by M.R. and C.T.M. All authors have read and agreed to the published version of the manuscript.

CONFLICTS OF INTEREST

The authors declare no conflicts of interest related to this study.

FUNDING

C. elegans strains used in this work were provided by the Caenorhabditis Genetics Centre (Univ. of Minnesota, USA), which is funded by NIH Office of Research Infrastructure Programs (P40 OD010440). Parts of this project are contained in a Ph.D. thesis (J.T., Effects and Mechanisms of Green Tea Polyphenols in Regards to Lifespan Extension, 2013, Friedrich Schiller University Jena, Germany) and a M.D. thesis (C.G., Pharmakologische Modulation der Lebenserwartung im Modellorganismus *Caenorhabditis elegans* durch Induktion des mitochondrialen Stoffwechsels, 2013, Friedrich Schiller University Jena, Germany). The Ristow laboratory has been supported by the Horizon 2020 program of the European Union (Ageing with Elegans, grant 633589) and is currently supported by the Swiss National Science Foundation (31003A_176127). C.T.M. is currently funded by an Erwin Schroedinger Abroad Fellowship (J4205-B27).

REFERENCES

1. Peng X, Zhou R, Wang B, Yu X, Yang X, Liu K, Mi M. Effect of green tea consumption on blood pressure: a meta-analysis of 13 randomized controlled trials. Sci Rep. 2014; 4:6251. https://doi.org/10.1038/srep06251 PMID:25176280

2. Xu R, Bai Y, Yang K, Chen G. Effects of green tea consumption on glycemic control: a systematic review and meta-analysis of randomized controlled trials. Nutr Metab (Lond). 2020; 17:56. https://doi.org/10.1186/s12986-020-00469-5 PMID:32670385

3. Mousavi A, Vafa M, Neyestani T, Khamseh M, Hoseini F. The effects of green tea consumption on metabolic and anthropometric indices in patients with Type 2 diabetes. J Res Med Sci. 2013; 18:1080–86. PMID:24523800

4. Chen IJ, Liu CY, Chiu JP, Hsu CH. Therapeutic effect of high-dose green tea extract on weight reduction: A randomized, double-blind, placebo-controlled clinical trial. Clin Nutr. 2016; 35:592–99. https://doi.org/10.1016/j.clnu.2015.05.003 PMID:26093535

5. Balentine DA, Wiseman SA, Bouwens LC. The chemistry of tea flavonoids. Crit Rev Food Sci Nutr. 1997; 37:693–704. https://doi.org/10.1080/10408399709527797 PMID:9447270

6. Jin Y, Jin CH, Row KH. Separation of catechin compounds from different teas. Biotechnol J. 2006; 1:209–13. https://doi.org/10.1002/biot.200500019 PMID:16892250

7. Kumar NB, Pow-Sang J, Spiess PE, Park J, Salup R, Williams CR, Parnes H, Schell MJ. Randomized, placebo-controlled trial evaluating the safety of one-year administration of green tea catechins. Oncotarget. 2016; 7:70794–802. https://doi.org/10.18632/oncotarget.12222 PMID:28053292

8. Andreu-Fernández V, Almeida Toledano L, Pizarro N, Navarro-Tapia E, Gómez-Roig MD, de la Torre R, García-Algar Ó. Bioavailability of Epigallocatechin Gallate Administered With Different Nutritional Strategies in Healthy Volunteers. Antioxidants (Basel). 2020; 9:440. https://doi.org/10.3390/antiox9050440 PMID:32438698

9. Wagner AE, Piegholdt S, Rabe D, Baenas N, Schloesser A, Eggersdorfer M, Stocker A, Rimbach G. Epigallocatechin gallate affects glucose metabolism and increases fitness and lifespan in Drosophila melanogaster. Oncotarget. 2015; 6:30568–78. https://doi.org/10.18632/oncotarget.5215 PMID:26375250

10. Kitani K, Osawa T, Yokozawa T. The effects of tetrahydrocurcumin and green tea polyphenol on the survival of male C57BL/6 mice. Biogerontology. 2007; 8:567–73. https://doi.org/10.1007/s10522-007-9100-z PMID:17516143

11. Xiong LG, Chen YJ, Tong JW, Gong YS, Huang JA, Liu ZH. Epigallocatechin-3-gallate promotes healthy lifespan through mitohormesis during early-to-mid adulthood in Caenorhabditis elegans. Redox Biol. 2018; 14:305–15. https://doi.org/10.1016/j.redox.2017.09.019 PMID:28992589

12. Zhu M, Chen Y, Li RC. Oral absorption and bioavailability of tea catechins. Planta Med. 2000; 66:444–47. https://doi.org/10.1055/s-2000-8599 PMID:10909265

13. Warden BA, Smith LS, Beecher GR, Balentine DA, Clevidence BA. Catechins are bioavailable in men and women drinking black tea throughout the day. J Nutr. 2001; 131:1731–37. https://doi.org/10.1093/jn/131.6.1731 PMID:11385060

14. Yang CS, Chen L, Lee MJ, Balentine D, Kuo MC, Schantz SP. Blood and urine levels of tea catechins after ingestion of different amounts of green tea by human volunteers. Cancer Epidemiol Biomarkers Prev. 1998; 7:351–54.
PMID:9568793

15. Rollins JA, Howard AC, Dobbins SK, Washburn EH, Rogers AN. Assessing Health Span in Caenorhabditis elegans: Lessons From Short-Lived Mutants. J Gerontol A Biol Sci Med Sci. 2017; 72:473–80.
https://doi.org/10.1093/gerona/glw248
PMID:28158466

16. Stefanatos R, Sanz A. Mitochondrial complex I: a central regulator of the aging process. Cell Cycle. 2011; 10:1528–32.
https://doi.org/10.4161/cc.10.10.15496
PMID:21471732

17. Mihaylova MM, Shaw RJ. The AMPK signalling pathway coordinates cell growth, autophagy and metabolism. Nat Cell Biol. 2011; 13:1016–23.
https://doi.org/10.1038/ncb2329
PMID:21892142

18. Schulz TJ, Zarse K, Voigt A, Urban N, Birringer M, Ristow M. Glucose restriction extends Caenorhabditis elegans life span by inducing mitochondrial respiration and increasing oxidative stress. Cell Metab. 2007; 6:280–93.
https://doi.org/10.1016/j.cmet.2007.08.011
PMID:17908557

19. Zarse K, Schmeisser S, Groth M, Priebe S, Beuster G, Kuhlow D, Guthke R, Platzer M, Kahn CR, Ristow M. Impaired insulin/IGF1 signaling extends life span by promoting mitochondrial L-proline catabolism to induce a transient ROS signal. Cell Metab. 2012; 15:451–65.
https://doi.org/10.1016/j.cmet.2012.02.013
PMID:22482728

20. Cantó C, Gerhart-Hines Z, Feige JN, Lagouge M, Noriega L, Milne JC, Elliott PJ, Puigserver P, Auwerx J. AMPK regulates energy expenditure by modulating NAD+ metabolism and SIRT1 activity. Nature. 2009; 458:1056–60.
https://doi.org/10.1038/nature07813
PMID:19262508

21. Torres M, Forman HJ. Redox signaling and the MAP kinase pathways. Biofactors. 2003; 17:287–96.
https://doi.org/10.1002/biof.5520170128
PMID:12897450

22. Lanna A, Henson SM, Escors D, Akbar AN. The kinase p38 activated by the metabolic regulator AMPK and scaffold TAB1 drives the senescence of human T cells. Nat Immunol. 2014; 15:965–72.
https://doi.org/10.1038/ni.2981
PMID:25151490

23. Pullikotil P, Chen H, Muniyappa R, Greenberg CC, Yang S, Reiter CE, Lee JW, Chung JH, Quon MJ. Epigallocatechin gallate induces expression of heme oxygenase-1 in endothelial cells via p38 MAPK and Nrf-2 that suppresses proinflammatory actions of TNF-α. J Nutr Biochem. 2012; 23:1134–45.
https://doi.org/10.1016/j.jnutbio.2011.06.007
PMID:22137262

24. Schmeisser S, Zarse K, Ristow M. Lonidamine extends lifespan of adult Caenorhabditis elegans by increasing the formation of mitochondrial reactive oxygen species. Horm Metab Res. 2011; 43:687–92.
https://doi.org/10.1055/s-0031-1286308
PMID:21932172

25. Inoue H, Hisamoto N, An JH, Oliveira RP, Nishida E, Blackwell TK, Matsumoto K. The C. elegans p38 MAPK pathway regulates nuclear localization of the transcription factor SKN-1 in oxidative stress response. Genes Dev. 2005; 19:2278–83.
https://doi.org/10.1101/gad.1324805
PMID:16166371

26. Kell A, Ventura N, Kahn N, Johnson TE. Activation of SKN-1 by novel kinases in Caenorhabditis elegans. Free Radic Biol Med. 2007; 43:1560–66.
https://doi.org/10.1016/j.freeradbiomed.2007.08.025
PMID:17964427

27. Yu R, Chen C, Mo YY, Hebbar V, Owuor ED, Tan TH, Kong AN. Activation of mitogen-activated protein kinase pathways induces antioxidant response element-mediated gene expression via a Nrf2-dependent mechanism. J Biol Chem. 2000; 275:39907–13.
https://doi.org/10.1074/jbc.M004037200
PMID:10986282

28. Ogg S, Paradis S, Gottlieb S, Patterson GI, Lee L, Tissenbaum HA, Ruvkun G. The Fork head transcription factor DAF-16 transduces insulin-like metabolic and longevity signals in C. elegans. Nature. 1997; 389:994–99.
https://doi.org/10.1038/40194
PMID:9353126

29. Murphy CT, McCarroll SA, Bargmann CI, Fraser A, Kamath RS, Ahringer J, Li H, Kenyon C. Genes that act downstream of DAF-16 to influence the lifespan of Caenorhabditis elegans. Nature. 2003; 424:277–83.
https://doi.org/10.1038/nature01789
PMID:12845331

30. Ristow M, Schmeisser K. Mitohormesis: Promoting Health and Lifespan by Increased Levels of Reactive Oxygen Species (ROS). Dose Response. 2014; 12:288–341.

https://doi.org/10.2203/dose-response.13-035.Ristow PMID:24910588

31. Petriv OI, Rachubinski RA. Lack of peroxisomal catalase causes a progeric phenotype in Caenorhabditis elegans. J Biol Chem. 2004; 279:19996–20001. https://doi.org/10.1074/jbc.M400207200 PMID:14996832

32. Zhao LG, Li HL, Sun JW, Yang Y, Ma X, Shu XO, Zheng W, Xiang YB. Green tea consumption and cause-specific mortality: Results from two prospective cohort studies in China. J Epidemiol. 2017; 27:36–41. https://doi.org/10.1016/j.je.2016.08.004 PMID:28135196

33. Basu A, Sanchez K, Leyva MJ, Wu M, Betts NM, Aston CE, Lyons TJ. Green tea supplementation affects body weight, lipids, and lipid peroxidation in obese subjects with metabolic syndrome. J Am Coll Nutr. 2010; 29:31–40. https://doi.org/10.1080/07315724.2010.10719814 PMID:20595643

34. Singh BN, Shankar S, Srivastava RK. Green tea catechin, epigallocatechin-3-gallate (EGCG): mechanisms, perspectives and clinical applications. Biochem Pharmacol. 2011; 82:1807–21. https://doi.org/10.1016/j.bcp.2011.07.093 PMID:21827739

35. Lambert JD, Elias RJ. The antioxidant and pro-oxidant activities of green tea polyphenols: a role in cancer prevention. Arch Biochem Biophys. 2010; 501:65–72. https://doi.org/10.1016/j.abb.2010.06.013 PMID:20558130

36. Elbling L, Herbacek I, Weiss RM, Gerner C, Heffeter P, Jantschitsch C, Trautinger F, Grusch M, Pangratz H, Berger W. EGCG-meditated cyto- and genotoxicity in HaCat keratinocytes is impaired by cell-mediated clearance of auto-oxidation-derived H2O2: an algorithm for experimental setting correction. Toxicol Lett. 2011; 205:173–82. https://doi.org/10.1016/j.toxlet.2011.06.001 PMID:21704138

37. Elbling L, Herbacek I, Weiss RM, Jantschitsch C, Micksche M, Gerner C, Pangratz H, Grusch M, Knasmüller S, Berger W. Hydrogen peroxide mediates EGCG-induced antioxidant protection in human keratinocytes. Free Radic Biol Med. 2010; 49:1444–52. https://doi.org/10.1016/j.freeradbiomed.2010.08.008 PMID:20708679

38. Li GX, Chen YK, Hou Z, Xiao H, Jin H, Lu G, Lee MJ, Liu B, Guan F, Yang Z, Yu A, Yang CS. Pro-oxidative activities and dose-response relationship of (-)-epigallocatechin-3-gallate in the inhibition of lung cancer cell growth: a comparative study in vivo and in vitro. Carcinogenesis. 2010; 31:902–10. https://doi.org/10.1093/carcin/bgq039 PMID:20159951

39. López-Lázaro M, Calderón-Montaño JM, Burgos-Morón E, Austin CA. Green tea constituents (-)-epigallocatechin-3-gallate (EGCG) and gallic acid induce topoisomerase I- and topoisomerase II-DNA complexes in cells mediated by pyrogallol-induced hydrogen peroxide. Mutagenesis. 2011; 26:489–98. https://doi.org/10.1093/mutage/ger006 PMID:21382914

40. Min NY, Kim JH, Choi JH, Liang W, Ko YJ, Rhee S, Bang H, Ham SW, Park AJ, Lee KH. Selective death of cancer cells by preferential induction of reactive oxygen species in response to (-)-epigallocatechin-3-gallate. Biochem Biophys Res Commun. 2012; 421:91–97. https://doi.org/10.1016/j.bbrc.2012.03.120 PMID:22487794

41. Yang GY, Liao J, Kim K, Yurkow EJ, Yang CS. Inhibition of growth and induction of apoptosis in human cancer cell lines by tea polyphenols. Carcinogenesis. 1998; 19:611–16. https://doi.org/10.1093/carcin/19.4.611 PMID:9600345

42. Bigelow RL, Cardelli JA. The green tea catechins, (-)-Epigallocatechin-3-gallate (EGCG) and (-)-Epicatechin-3-gallate (ECG), inhibit HGF/Met signaling in immortalized and tumorigenic breast epithelial cells. Oncogene. 2006; 25:1922–30. https://doi.org/10.1038/sj.onc.1209227 PMID:16449979

43. Higdon JV, Frei B. Tea catechins and polyphenols: health effects, metabolism, and antioxidant functions. Crit Rev Food Sci Nutr. 2003; 43:89–143. https://doi.org/10.1080/10408690390826464 PMID:12587987

44. Abbas S, Wink M. Epigallocatechin gallate from green tea (Camellia sinensis) increases lifespan and stress resistance in Caenorhabditis elegans. Planta Med. 2009; 75:216–21. https://doi.org/10.1055/s-0028-1088378 PMID:19085685

45. Crozier A, Jaganath IB, Clifford MN. Dietary phenolics: chemistry, bioavailability and effects on health. Nat Prod Rep. 2009; 26:1001–43. https://doi.org/10.1039/b802662a PMID:19636448

46. Schafer FQ, Buettner GR. Redox environment of the cell as viewed through the redox state of the

glutathione disulfide/glutathione couple. Free Radic Biol Med. 2001; 30:1191–212. https://doi.org/10.1016/s0891-5849(01)00480-4 PMID:11368918

47. Back P, Braeckman BP, Matthijssens F. ROS in aging Caenorhabditis elegans: damage or signaling? Oxid Med Cell Longev. 2012; 2012:608478. https://doi.org/10.1155/2012/608478 PMID:22966416

48. Bartholome A, Kampkötter A, Tanner S, Sies H, Klotz LO. Epigallocatechin gallate-induced modulation of FoxO signaling in mammalian cells and C. elegans: FoxO stimulation is masked via PI3K/Akt activation by hydrogen peroxide formed in cell culture. Arch Biochem Biophys. 2010; 501:58–64. https://doi.org/10.1016/j.abb.2010.05.024 PMID:20513639

49. Suh KS, Chon S, Oh S, Kim SW, Kim JW, Kim YS, Woo JT. Prooxidative effects of green tea polyphenol (-)-epigallocatechin-3-gallate on the HIT-T15 pancreatic beta cell line. Cell Biol Toxicol. 2010; 26:189–99. https://doi.org/10.1007/s10565-009-9137-7 PMID:19757103

50. Chen C, Shen G, Hebbar V, Hu R, Owuor ED, Kong AN. Epigallocatechin-3-gallate-induced stress signals in HT-29 human colon adenocarcinoma cells. Carcinogenesis. 2003; 24:1369–78. https://doi.org/10.1093/carcin/bgg091 PMID:12819184

51. Wang CT, Chang HH, Hsiao CH, Lee MJ, Ku HC, Hu YJ, Kao YH. The effects of green tea (-)-epigallocatechin-3-gallate on reactive oxygen species in 3T3-L1 preadipocytes and adipocytes depend on the glutathione and 67 kDa laminin receptor pathways. Mol Nutr Food Res. 2009; 53:349–60. https://doi.org/10.1002/mnfr.200800013 PMID:19065584

52. Schroeder EK, Kelsey NA, Doyle J, Breed E, Bouchard RJ, Loucks FA, Harbison RA, Linseman DA. Green tea epigallocatechin 3-gallate accumulates in mitochondria and displays a selective antiapoptotic effect against inducers of mitochondrial oxidative stress in neurons. Antioxid Redox Signal. 2009; 11:469–80. https://doi.org/10.1089/ars.2008.2215 PMID:18754708

53. Gorlach S, Fichna J, Lewandowska U. Polyphenols as mitochondria-targeted anticancer drugs. Cancer Lett. 2015; 366:141–49. https://doi.org/10.1016/j.canlet.2015.07.004 PMID:26185003

54. Teixeira J, Chavarria D, Borges F, Wojtczak L, Wieckowski MR, Karkucinska-Wieckowska A, Oliveira PJ. Dietary Polyphenols and Mitochondrial Function: Role in Health and Disease. Curr Med Chem. 2019; 26:3376–406. https://doi.org/10.2174/0929867324666170529101810 PMID:28554320

55. Heller A, Brockhoff G, Goepferich A. Targeting drugs to mitochondria. Eur J Pharm Biopharm. 2012; 82:1–18. https://doi.org/10.1016/j.ejpb.2012.05.014 PMID:22687572

56. Frantz MC, Wipf P. Mitochondria as a target in treatment. Environ Mol Mutagen. 2010; 51:462–75. https://doi.org/10.1002/em.20554 PMID:20175113

57. Picard M, Taivassalo T, Gouspillou G, Hepple RT. Mitochondria: isolation, structure and function. J Physiol. 2011; 589:4413–21. https://doi.org/10.1113/jphysiol.2011.212712 PMID:21708903

58. Yang W, Hekimi S. A mitochondrial superoxide signal triggers increased longevity in Caenorhabditis elegans. PLoS Biol. 2010; 8:e1000556. https://doi.org/10.1371/journal.pbio.1000556 PMID:21151885

59. Yang W, Hekimi S. Two modes of mitochondrial dysfunction lead independently to lifespan extension in Caenorhabditis elegans. Aging Cell. 2010; 9:433–47. https://doi.org/10.1111/j.1474-9726.2010.00571.x PMID:20346072

60. Hekimi S, Burgess J, Bussière F, Meng Y, Bénard C. Genetics of lifespan in C. elegans: molecular diversity, physiological complexity, mechanistic simplicity. Trends Genet. 2001; 17:712–18. https://doi.org/10.1016/s0168-9525(01)02523-9 PMID:11718925

61. Lakowski B, Hekimi S. Determination of life-span in Caenorhabditis elegans by four clock genes. Science. 1996; 272:1010–13. https://doi.org/10.1126/science.272.5264.1010 PMID:8638122

62. Branicky R, Bénard C, Hekimi S. clk-1, mitochondria, and physiological rates. Bioessays. 2000; 22:48–56. https://doi.org/10.1002/(SICI)1521-1878(200001)22:1<48::AID-BIES9>3.0.CO;2-F PMID:10649290

63. Tsang WY, Lemire BD. Mitochondrial genome content is regulated during nematode development. Biochem Biophys Res Commun. 2002; 291:8–16. https://doi.org/10.1006/bbrc.2002.6394 PMID:11829454

64. Dillin A, Hsu AL, Arantes-Oliveira N, Lehrer-Graiwer J, Hsin H, Fraser AG, Kamath RS, Ahringer J, Kenyon C.

Rates of behavior and aging specified by mitochondrial function during development. Science. 2002; 298:2398–401. https://doi.org/10.1126/science.1077780 PMID:12471266

65. Rea SL, Ventura N, Johnson TE. Relationship between mitochondrial electron transport chain dysfunction, development, and life extension in Caenorhabditis elegans. PLoS Biol. 2007; 5:e259. https://doi.org/10.1371/journal.pbio.0050259 PMID:17914900

66. Woo DK, Shadel GS. Mitochondrial stress signals revise an old aging theory. Cell. 2011; 144:11–12. https://doi.org/10.1016/j.cell.2010.12.023 PMID:21215364

67. Durieux J, Wolff S, Dillin A. The cell-non-autonomous nature of electron transport chain-mediated longevity. Cell. 2011; 144:79–91. https://doi.org/10.1016/j.cell.2010.12.016 PMID:21215371

68. Zhang L, Jie G, Zhang J, Zhao B. Significant longevity-extending effects of EGCG on Caenorhabditis elegans under stress. Free Radic Biol Med. 2009; 46:414–21. https://doi.org/10.1016/j.freeradbiomed.2008.10.041 PMID:19061950

69. Bishop NA, Guarente L. Two neurons mediate diet-restriction-induced longevity in C. elegans. Nature. 2007; 447:545–49. https://doi.org/10.1038/nature05904 PMID:17538612

70. Tullet JM, Hertweck M, An JH, Baker J, Hwang JY, Liu S, Oliveira RP, Baumeister R, Blackwell TK. Direct inhibition of the longevity-promoting factor SKN-1 by insulin-like signaling in C. elegans. Cell. 2008; 132:1025–38. https://doi.org/10.1016/j.cell.2008.01.030 PMID:18358814

71. Murphy CT. The search for DAF-16/FOXO transcriptional targets: approaches and discoveries. Exp Gerontol. 2006; 41:910–21. https://doi.org/10.1016/j.exger.2006.06.040 PMID:16934425

72. Oh SW, Mukhopadhyay A, Dixit BL, Raha T, Green MR, Tissenbaum HA. Identification of direct DAF-16 targets controlling longevity, metabolism and diapause by chromatin immunoprecipitation. Nat Genet. 2006; 38:251–57. https://doi.org/10.1038/ng1723 PMID:16380712

73. Li J, Miller EJ, Ninomiya-Tsuji J, Russell RR 3rd, Young LH. AMP-activated protein kinase activates p38 mitogen-activated protein kinase by increasing recruitment of p38 MAPK to TAB1 in the ischemic heart. Circ Res. 2005; 97:872–79. https://doi.org/10.1161/01.RES.0000187458.77026.10 PMID:16179588

74. McKay RM, McKay JP, Avery L, Graff JM. C elegans: a model for exploring the genetics of fat storage. Dev Cell. 2003; 4:131–42. https://doi.org/10.1016/s1534-5807(02)00411-2 PMID:12530969

75. Liu J, Peng Y, Yue Y, Shen P, Park Y. Epigallocatechin-3-Gallate Reduces Fat Accumulation in *Caenorhabditis elegans*. Prev Nutr Food Sci. 2018; 23:214–19. https://doi.org/10.3746/pnf.2018.23.3.214 PMID:30386749

76. Hasumura T, Shimada Y, Kuroyanagi J, Nishimura Y, Meguro S, Takema Y, Tanaka T. Green tea extract suppresses adiposity and affects the expression of lipid metabolism genes in diet-induced obese zebrafish. Nutr Metab (Lond). 2012; 9:73. https://doi.org/10.1186/1743-7075-9-73 PMID:22871059

77. Li F, Gao C, Yan P, Zhang M, Wang Y, Hu Y, Wu X, Wang X, Sheng J. EGCG Reduces Obesity and White Adipose Tissue Gain Partly Through AMPK Activation in Mice. Front Pharmacol. 2018; 9:1366. https://doi.org/10.3389/fphar.2018.01366 PMID:30524290

78. Lu C, Zhu W, Shen CL, Gao W. Green tea polyphenols reduce body weight in rats by modulating obesity-related genes. PLoS One. 2012; 7:e38332. https://doi.org/10.1371/journal.pone.0038332 PMID:22715380

79. Kao YH, Chang HH, Lee MJ, Chen CL. Tea, obesity, and diabetes. Mol Nutr Food Res. 2006; 50:188–210. https://doi.org/10.1002/mnfr.200500109 PMID:16416476

80. Thielecke F, Boschmann M. The potential role of green tea catechins in the prevention of the metabolic syndrome - a review. Phytochemistry. 2009; 70:11–24. https://doi.org/10.1016/j.phytochem.2008.11.011 PMID:19147161

81. Grove KA, Lambert JD. Laboratory, epidemiological, and human intervention studies show that tea (Camellia sinensis) may be useful in the prevention of obesity. J Nutr. 2010; 140:446–53. https://doi.org/10.3945/jn.109.115972 PMID:20089791

82. Brenner S. The genetics of Caenorhabditis elegans. Genetics. 1974; 77:71–94. https://doi.org/10.1093/genetics/77.1.71 PMID:4366476

83. Byerly L, Scherer S, Russell RL. The life cycle of the nematode Caenorhabditis elegans. II. A simplified method for mutant characterization. Dev Biol. 1976; 51:34–48.
https://doi.org/10.1016/0012-1606(76)90120-2
PMID:988846

84. Schmeisser S, Priebe S, Groth M, Monajembashi S, Hemmerich P, Guthke R, Platzer M, Ristow M. Neuronal ROS signaling rather than AMPK/sirtuin-mediated energy sensing links dietary restriction to lifespan extension. Mol Metab. 2013; 2:92–102.
https://doi.org/10.1016/j.molmet.2013.02.002
PMID:24199155

85. Dresen A, Finkbeiner S, Dottermusch M, Beume JS, Li Y, Walz G, Neumann-Haefelin E. Caenorhabditis elegans OSM-11 signaling regulates SKN-1/Nrf during embryonic development and adult longevity and stress response. Dev Biol. 2015; 400:118–31.
https://doi.org/10.1016/j.ydbio.2015.01.021
PMID:25637691

86. Bradford MM. A rapid and sensitive method for the quantitation of microgram quantities of protein utilizing the principle of protein-dye binding. Anal Biochem. 1976; 72:248–54.
https://doi.org/10.1006/abio.1976.9999
PMID:942051

87. Weimer S, Priebs J, Kuhlow D, Groth M, Priebe S, Mansfeld J, Merry TL, Dubuis S, Laube B, Pfeiffer AF, Schulz TJ, Guthke R, Platzer M, et al. D-Glucosamine supplementation extends life span of nematodes and of ageing mice. Nat Commun. 2014; 5:3563.
https://doi.org/10.1038/ncomms4563
PMID:24714520

88. Ristow M, Pfister MF, Yee AJ, Schubert M, Michael L, Zhang CY, Ueki K, Michael MD 2nd, Lowell BB, Kahn CR. Frataxin activates mitochondrial energy conversion and oxidative phosphorylation. Proc Natl Acad Sci U S A. 2000; 97:12239–43.
https://doi.org/10.1073/pnas.220403797
PMID:11035806

89. Kumsta C, Thamsen M, Jakob U. Effects of oxidative stress on behavior, physiology, and the redox thiol proteome of Caenorhabditis elegans. Antioxid Redox Signal. 2011; 14:1023–37.
https://doi.org/10.1089/ars.2010.3203
PMID:20649472

90. Janssen AJ, Trijbels FJ, Sengers RC, Smeitink JA, van den Heuvel LP, Wintjes LT, Stoltenborg-Hogenkamp BJ, Rodenburg RJ. Spectrophotometric assay for complex I of the respiratory chain in tissue samples and cultured fibroblasts. Clin Chem. 2007; 53:729–34.
https://doi.org/10.1373/clinchem.2006.078873
PMID:17332151

91. Frezza C, Cipolat S, Scorrano L. Organelle isolation: functional mitochondria from mouse liver, muscle and cultured fibroblasts. Nat Protoc. 2007; 2:287–95.
https://doi.org/10.1038/nprot.2006.478
PMID:17406588